

Ultra-Thin Piezoelectric Film Optimization

Spring 2017 Semester Projects

Lausanne, Date: 09.06.2017

Student :
Tamara Miteva

Professor:
Prof. Dr. Guillermo Villanueva
Assistant:
Kaitlin Howell

Table of Contents

Ultra-thin Piezoelectric film optimization	1
Spring 2017 Semester Projects	1
1 Introduction	3
2 Theory	4
2.1 Magnetron DC sputtering.....	4
2.2 Thin film growth	5
2.3 Material science	6
2.4 Piezoelectricity, strain and deflection of ALN	7
3 Microfabrication	8
3.1 Methods of deposition.....	8
3.2 Prepare step of wafers before deposition.....	9
3.3 1 st set of depositions.....	9
3.4 2 nd set of depositions	10
4 Measurement methods	10
4.1 Sopra GES 5E	10
4.2 NanoSpec AFT-6100.....	11
4.3 Bruker Dektak XT.....	11
.....	12
4.4 Toho technology FLX 2320-S.....	12
4.5 KLA Tencor OmniMap RS75.....	13
4.6 XRD.....	13
4.7 Procedure for measuring thickness	14
5 Results	16
5.1 Results of thickness measurements.....	16
5.2 Results of stress measurements	17
5.3 Results of resistance and resistivity measurements	19
5.4 Results of XRD measurement	20
6 Discussion	21
7 Conclusion	22

1 INTRODUCTION

Ultra-thin piezoelectric films are important matter of the modern technology. The main application is in the electronic industry but they are also widely used in research. The emphasis of this project is set to platinum and aluminium nitride thin films optimization. The largest piezoelectricity coefficients of aluminium nitride thin films are obtained with platinum substrate. Platinum is frequently the material of choice in microelectronics. The substrate and the deposition process significantly influence the growth and the properties of the aluminium nitride thin films. [1] Namely, finding the “best” platinum thin-film, will provide the “best quality” active aluminium nitride ultra-thin film growth on top of it. Regarding to that, aluminium nitride thin films were deposited on platinum by changing the processing conditions of platinum layer substrate, by DC magnetron sputtering. We studied the thickness, the stress and the resistivity of the platinum layer as function of some processing conditions. Eventually, X-ray diffraction measurements were performed on each wafer to check the crystallinity of the aluminium nitride thin film. Shrinking the number of conductivity electrons relates to reduced conductivity of the thin film and it is caused at rough surfaces [2] and interfaces [3] and at grain boundaries [4]. The resistivity and the residual stress in thin-films is disadvantageous. In order to obtain the thickness, stress and resistivity of platinum layer, different series of measurements were completed through the depositions. The results from the measurements are presented through graphical plots and are discussed additionally. At the end of the semester project, we had fourteen different deposited wafers. Our work is oriented toward understanding the influence of some of the deposit parameters, particularly the power and the gas flow, to the thin films quality. Piezoelectric thin films based on aluminum nitride are highly interesting for their robust mechanical thermal properties, as well as high electrical resistance and breakdown voltage. The quality of the aluminum nitride thin film is the key of various applications and industrial devices. Aluminum nitride have been used for applications such as surface acoustic wave (SAW) devices, film bulk acoustic wave resonators (FBARs) and RF filters. Piezoelectric layers based on aluminum nitride have been demonstrated to be useful thus the range of MEMS applications is enormously large. Our aim is to obtain reproducible nanometer thick aluminum nitride films on metallic surfaces with consistently stable thin film deposition. Regarding to that, manipulating the sputtering by modifying several deposition parameters for having small deposition rate and conducting analysis of the results for the thin films parameters, we demonstrate what will happen every time when we repeat the same procedure. The parameters that most influence the deposition are: the target power, the gas flow or the target-substrate distance. At the beginning of this project the theory and papers that do similar work were reviewed in terms of getting better idea what was already accomplished. Furthermore, after learning the theory, I trained how to use some of the machines in the cleanroom that were necessary for doing the growing layers fabrication and making the measurements. I learned how to use the metrology machines as: Omnimap (measure the square resistance and uniformity), XRD (measuring the crystallinity), Toho

(measuring the residual stress) and Dektak profilometer (measuring the thickness). Through the work in the cleanroom, several sets of depositions were performed for which only one sputtering parameter was changed and all the others were kept constant. According to that, we investigated the influence of the parameters we change during the deposition on the properties of the aluminum nitride and platinum thin films. In the 1st deposition set, we deposited seed aluminum nitride, platinum, active aluminum nitride and aluminum layers in two deposition steps on ten wafers by changing the sputtering conditions for only the platinum layer. All other layers were deposited with same conditions on each wafer. The layer of aluminum nitride underneath the platinum layer is used as isolator. The layer of aluminum nitride on top of the platinum layer is the active piezoelectric layer and the one of our interest. The 2nd set of depositions was performed, because of the odd results for gas flows of 10 and 15 [sccm]. Out of curiosity we redeposit these two specific wafers one more time to see if we encounter same results. The only difference is that we used titanium instead aluminum nitride as isolator beneath the Pt layer. Papers on this subject that investigate the quality of the layers did not try to change this specific processing parameters: the power and the gas flow.

2 THEORY

2.1 Magnetron DC sputtering

Tons technologies for forming thin layers of materials occur today and enable us to use variety of deposition techniques. MEMS deposition technology can be categorized as depositions that take place because of chemical reaction (chemical vapor deposition, electrodeposition, epitaxy, thermal oxidation) or depositions that take place because of physical reaction (physical vapor deposition and casting). The two most important technologies are evaporation and sputtering. Our main interest, in this project, is in the sputtering technique. [5] There are two main sputtering techniques: the DC and RF sputtering. The magnetron DC sputtering is the technique that we used for fabrication of the thin layers. In DC sputtering

(diode discharge), the sputtering target is placed on the cathode electrode and the substrate on the anode, which is often at ground potential or positively biased, as presented in figure 1. A DC voltage is applied between the target and substrate which ionizes argon atoms and crates plasma (consisted of ions and electrons). These ionized argon atoms are accelerated to the cathode (target) as presented on figure 2. The method of separating the atoms of interest from the bulk material

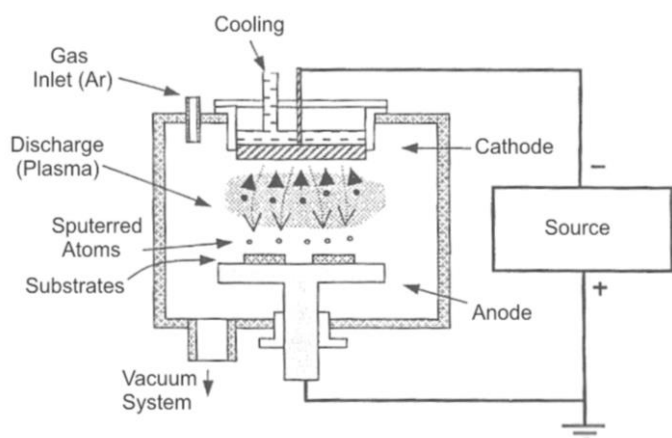


Figure 1. Magnetron DC sputtering chamber

carrying it in magnetron DC sputtering is purely physical and no chemical processes that forms the thin film is taking place. Sputtering is a physical vapor deposition process where the atoms of the target material, inside the vacuum chamber, are ejected due to bombardment of the target by energetic particles (gas ions). The bombardment of the target material is feasible because the applied potential appears across a region very near the cathode which generates the plasma discharge between two electrodes in a vacuum chamber. The discharge is generated when pressure and a sputter argon gas is applied inside the chamber. The plasma bombardment cause the target material of our interest to travel some distance and eventually reach the substrate and form thin layer consisted of the target material. As more atoms reach the substrate more material is deposited. If we have insulating target material installed on the cathode, there will be a surface charge that will prevent ion bombardment of the surface, thus electrical conductor (such as metals) is used. [6] The electrons that are ejected from the target material are accelerated away from the cathode and are not efficiently used for sustaining the discharge (plasma). The magnetron DC sputtering system, includes magnetron to enhance the process and increase the probability of further ionizing argon atoms (more electrons that take place in ionization event) and therefore produce stable high density plasma. Otherwise large part of the secondary electrons emitted by the target do not cause ionization of argon. [7] Another reason to use magnets are: lower voltage needed to produce the plasma, controls uniformity and increases deposition rate. With the magnetron, we force the electrons to move on a specific target surface path. Moreover, working in vacuum provides longer mean free path, in such a way that provides time for the reactants to react and form the thin film. Though the basic idea of the magnetron DC sputtering process looks simple, it is very complex because of the influence of various parameters included in the process. The deposited thin films can be controlled through changing huge number of parameters in the deposition machine.

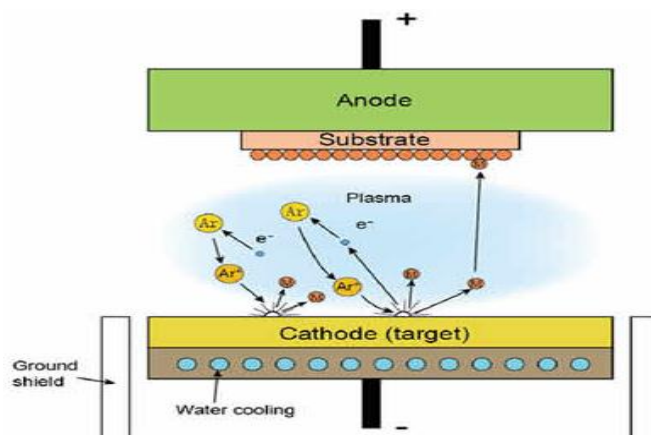


Figure 2. Basic idea of DC magnetron sputtering

2.2 Thin film growth

The growth of thin films depends on the deposition temperature, the interface energy and the lattice mismatch between target and substrate. The three basic physical modes are known as:

a) Volmer–Weber model (island) b) Frank van der Merwe model (layer) and c) Stranski–Krastanov model(layer plus island), shown on figure 3. [8]

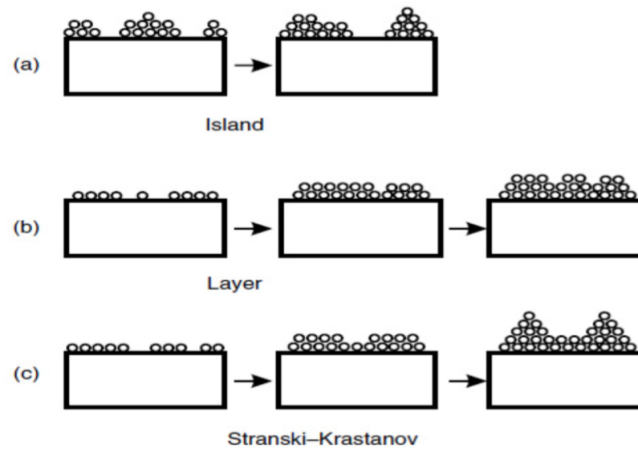


Figure 3. Three mechanisms of nucleation and growth of thin films

For producing a stable film, one need nuclei at critical size. The formation of such stable nuclei is called nucleation (film growth). In Volmer–Weber model (island), the film growth is uneven. Moreover the number of nuclei and the size of a given nucleus increase simultaneously. The nuclei grow until they mix with each other to form a continuous film. In the Frank- Vander Merwe model a smooth layer will be formed and layer growth will occur. (in layer by layer manner). The Stransky and Krastanov (mixed) model combines the layer growth and island nucleation. In this nucleation, the growth is uneven.

2.3 Material science

In this project, among other things it is significant to know the structure and the properties of the materials that we are using (Pt, AlN, Al, SiO₂). A lot of properties of the materials depends on the crystal structure: the strength, the conductivity, the speed of light etc. Crystalline (“morphus”) material has it is atoms packed in periodic 3D arrays. On the other hand, the non-crystalline (“amorphous”) materials occurs in a complex structure and the atoms have no periodic packing. Solids are either crystalline or non-crystalline. Diverse piezoelectric materials are recognized (as quartz crystals, ceramics etc.). However only few are utilized for installation in MEMS devices as aluminum nitride, PZT, zinc oxide (ZnO), lithium niobate and lead magnesium niobate-lead titanate. Currently, AlN and PZT show the best fusion of coupling factor, mechanical quality and ease of deposition. [9] Even though PZT is most promising in terms of converting mechanical to electrical energy (best for MEMS power generation), we choice aluminum nitride because of its great potential especially in MEMS resonators in terms of acoustic properties, piezoelectric properties, high thermal conductivity and good compatibility with other electronic technologies. [10] [11] Since the largest piezoelectricity coefficients of aluminium nitride thin films are obtained with platinum substrate, the bottom electrode is from platinum. [12] The hexagonal crystal lattice of

aluminium nitride is shown on figure 4 (left) and the FCC(face-centered cubic) crystal structure on figure 4 (right).

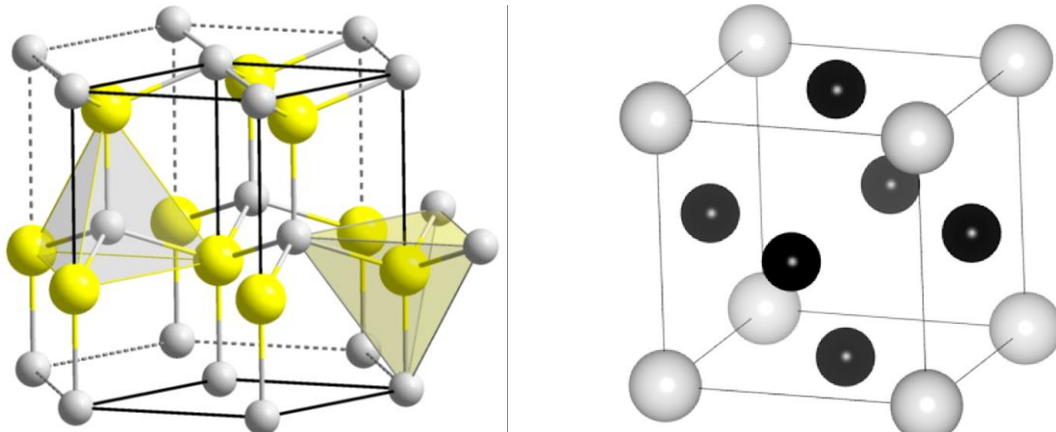


Figure 4. Crystal lattice of AlN (left) and Pt (right)

2.4 Piezoelectricity, strain and deflection of ALN

Piezoelectricity is an exciting field of Micro and Nano technology, since it gathers strain by the application of electric field and vice versa. The piezoelectric phenomenon was discovered in 1880 by French physicists Jacques and Pierre Curie. [13] The piezoelectric coefficients are used to describe the piezoelectricity property of the piezoelectric layer (aluminum nitride). The current is applied on the piezoelectric aluminum nitride layer. That is exactly the layer that induces the electricity and strain on both sides up (top electrode) and down on it (bottom electrode). If we have just one layer of aluminum on top of it and the same layer of aluminum below it, then deflection will not appear, because the geometrical center (neutral center) of the three layers and the piezoelectric center are colliding. The deflection will not appear since we added layers with same properties and with same thickness. Thus, in our case we are depositing different layers of materials with different thickness below and above the aluminum nitride layer, to have different strain up and below the active aluminum nitride layer. In this case, because of the different strain, our wafer tends to go in equilibrium position and it bends to do that. By applying this different layer from different materials and different thicknesses, we are inducing the deflection. This principal is very similar as the thermal case, where we induce the deflection by changing the temperature of the layers. Only here we induce the deflection by making different thickness of layers on top and below the piezoelectric layer. This will make the centers for the neutral center (geometrical center) of the wafer and the piezoelectric center to be different. From structural mechanics, if the change between this two axes is zero there will be no deflection. Otherwise we can calculate the deflection with knowing this change in the axes, the geometrical properties of the wafer (the length), the piezo resistive coefficient and the material properties (Young modulus and the inertia).

3 MICROFABRICATION

3.1 Methods of deposition

All depositions were fulfilled using the deposition machine: SPIDER 600 placed in Zone 4 in the clean room of the center of micronanotechnology and its user interface is shown on figure 5. The SPIDER equipment was used for depositing all the materials we used in this project. The deposition material can be a pure metal, An alloy or a dielectric material. [14] Before performing the deposition, we managed to look inside the machine and follow the procedure of changing the target material in terms of better understanding the DC magnetron sputtering process. We observed, on top of each chamber there is one target (rectangular plate) and on top of each target there is a magnetron. The SPIDER has four independent deposition chambers (or process modules), one central chamber for exchanging wafers with help of a robot arm and one load lock. The robot arm transfers the wafers from the load locker to some of the chambers or from one chamber to another.

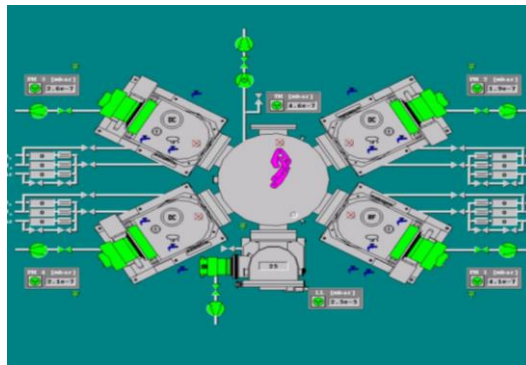


Figure 5. Spider deposition machine user interface

Firstly, before depositing the thin films, we cleaned the target under vacuum by ion bombardment with “trash” wafers. Cleaning the vacuum target just prior to deposition is essential to ensure good layer quality. This cleaning process takes some time and it is important to take this in account when booking the machine. In the 1st depositions set, we deposited four layers: seed aluminum nitride, platinum, active aluminum nitride and aluminum layers, on ten wafers by changing the sputtering conditions for only the platinum layer. The deposition was accomplished in two steps, firstly we deposited the bottom two layers and then after doing certain measurements the top two layers. Furthermore, RF etch was introduced for cleaning the surface of platinum layer before depositing the top two layers of active aluminum nitride and aluminum. Changing some of the sputtering parameters in the Spider machine, requires consultations and permeation from the staff in the clean room. With this in mind, we had a meeting with Dr. Philippe Langlet and he explained that is not realizable to manually change the target-substrate distance in the Spider machine which lead us to change in other two parameters that most influence the deposition: the target power and the gas flow.

3.2 Prepare step of wafers before deposition

The preparation step is essential in terms of having a successful deposition. Generally, in the cleanroom, the deposition take always more time than you plan either because of technical problems with the machine or problems with the recipe. By preparing the wafers and by planning all the things that we need to do step by step, we can at least try to avoid problems that are caused by us, the users of the machine. We learned that we need to remember to do the following preparation steps:

- Measure SiO₂ thickness on NanoSpec
- Measure the curvature of the Si wafer with Toho
- Put tape and ink
- Plan how much time we need for depositing the layers and book the machine for

3.3 1st set of depositions

In the 1st set of depositions we deposited four layers on each of the following ten wafers, presented in figure 6, obtained as function of three different powers: 500 [W], 750 [W] and 1000 [W] and three different gas flows: 5 [sccm], 10 [sccm] and 15 [sccm] for the platinum layer. As we already mentioned, the other three layers are all deposited with the same deposition conditions, presented in detail in the appendix. We deposited active aluminum nitride layer of 100 [nm] and the aluminum layer of 100 [nm] and assumed the same total thickness of this top two layers with its standard deviation for all the wafers: $t_{AlN+Al} = 200 \pm 5$ [nm]. The deposition time for the platinum layer is fixed to 1 min. The range of powers between 500 and 1000 [W] was suggestion from Dr.Philippe Langlet as regime that will give stable deposition whit results that will happen every time with certain error. In contrast, if we hit the extremes the results can't be reproducible.

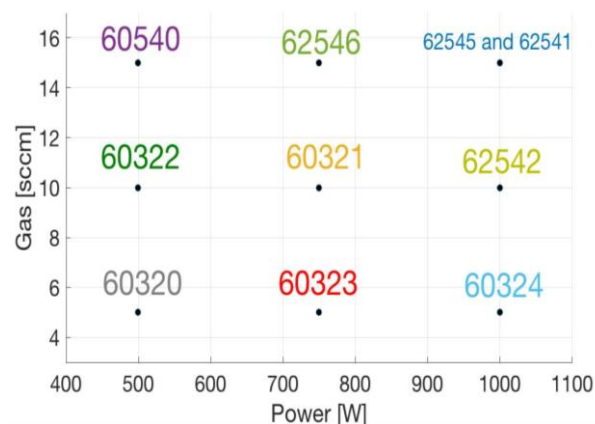


Figure 6. Number of wafers as function of power and gas flow for

Moreover, additional two wafers, with wafer number 62539 and 62543 were deposited with only aluminum nitride layer. In the 2nd set of depositions, we redeposited two wafers with

number 68135 and 68136, with seed titanium, platinum, active aluminum nitride and aluminum layers for checking the accuracy of the previous results. Furthermore, the list with the recipe names and deposition conditions for each wafer used in Spider machine are given in appendix. The two layers of seed aluminum nitride and platinum are deposited in one deposition step (cluster deposition). Firstly, depositing these two layers in one step together is significant, because of contamination reasons, which can possibly cause change in the properties of the deposited layers. Secondly, aluminum nitride forms oxide thus if we took it out of the Spider machine, the deposited platinum on top of it would not have the same quality. Then again if we don't deposit these two layers at once, we lose a lot of qualities. In the best case scenario, we would've deposited all the four layers of aluminum nitride, platinum, aluminum nitride and aluminum all together. But since our aim is to measure the platinum thickness, we performed two deposition steps of two by two layers. Since no opportunity exists for single layer measurements, for cluster deposition, the following strategy is realized: tape and ink is applied before and removed after the deposition of the two layers of aluminum nitride and platinum and the profile of the surface (the step of these two layers) is measured. For calculating the platinum thickness, one needs to extract the aluminum nitride thickness from the measured step. The thickness of the additional two wafers with only aluminum nitride deposited layers is measured and since the aluminum nitride layer is deposited with the same condition on each wafer we assume the same thickness on each of the wafers. During the deposition of the aluminum nitride layer, the reflected power must be zero, because otherwise we may have a problem with the machine or the recipe and we can possibly end up with a bad quality of the aluminum nitride layer. For some of the wafers deposited with the four layers, an improved and quicker recipe was made to decrease overall machine usage.

3.4 2nd set of depositions

In the 2nd set of depositions we redeposited four layers (now instead of seed AlN we have Ti layer) on each of the two wafers deposited on different gas flows: 5 [sccm], 10 [sccm] and on constant power of 500 [W] for the platinum layer. The other layers are deposited with the same conditions.

4 MEASUREMENT METHODS

4.1 Sopra GES 5E

The spectroscopic ellipsometer, Sopra Ges 5e, shown in figure 7, is placed in zone 3 in the clean room and is used to measure the thicknesses and refractive indices of transparent or optically absorbent thin layers. We used it for measuring the thickness of the aluminum nitride layer on wafers number: 62339 and 62543. [15] The measured

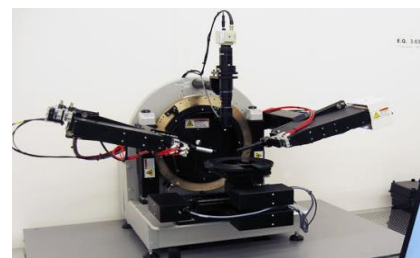


Figure 7. Sopra GES 5E

thickness of the aluminum nitride layer, on the two only aluminum nitride layer wafers is:

$$\begin{aligned}t_{AlN(62539)} &= 18,20 \pm 0,19 \text{ [nm]} \\t_{AlN(62543)} &= 18,77 \pm 0,22 \text{ [nm]}\end{aligned}\tag{1}$$

4.2 NanoSpec AFT-6100

NanoSpec, shown on figure 8, is spectroscopic reflectometer which is placed in zone 3 inside the clean room. We used this metrology machine for measuring the thickness of SiO₂ layer on each wafer before depositing the layers. To measure the thickness of SiO₂ layer, with NanoSpec, we used recipe number 157. This recipe automatically measure 48 pts on each wafer and gives us the minimum and maximum values, the standard deviation, the uniformity and the average value of the thickness of the SiO₂ layer. For wafers number 62540,62545 and 62546, we used recipe which measure the thickness of SiO₂ on one place only, because we didn't know yet about recipe number 157 hence we measured the thickness on 4 pts and calculated manually the average and STD. The values from the measurements are presented in the appendix. After the depositions, we premeasured the thickness of SiO₂ layer on Nanospec, and for all 10 wafer the value was around 280 [nm] with certain tolerance, which proved us that the tape and the ink did not took out the SiO₂ layer.



Figure 8. NanoSpec AFT -6100

4.3 Bruker Dektak XT

The surface profiler, Dektak, shown on figure 9 is placed in zone 4 inside the clean room. Dektak has a moving cantilever with a tip (stylus) on it. We used the machine for measuring the total thickness of the two layers of aluminum nitride and platinum, by doing four measurements on each wafer. This machine is measuring the step while running gently across the surface of the wafer with the stylus, following the profile of the surface (the hills and valleys) and the results, shown on figure 10 and 1,



Figure 9. Dektak profilometer

are presented though graphs on computer interface. As shown on figure 11, for some of the wafers there was appearing peak, which influenced the accuracy of the measured step. Dektak profilometer is very sensitive to any movement in its environment. The external protective box need to be closed because otherwise the tip can be easily disturbed and can lead to incorrect

result in the measurements. At the middle of our project, Dektak was broken, due to a technical error, and we continued the measurements on another profilometer machine called FlexScan L565.

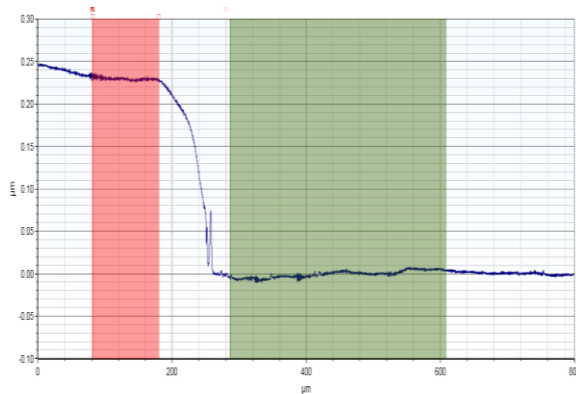


Figure 11. Dektak measurement of wafer 62546, resolution 0,044.

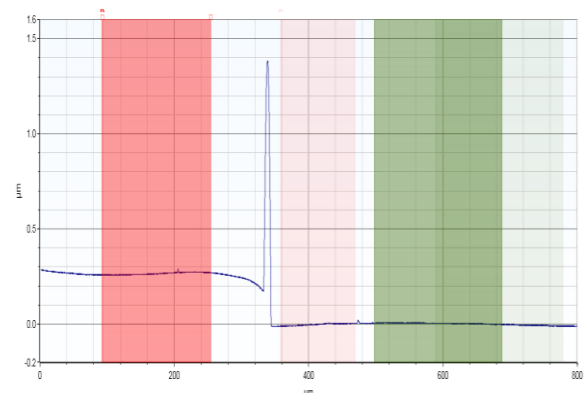


Figure 10. Measured step for wafer number 60321, resolution 0,044.

4.4 Toho technology FLX 2320-S

The film stress measurement tool, Toho technology FLX 2320-S, shown on figure 12, is placed in zone 11, at the +1 floor in the clean room. It uses a laser interferometer to measure the radius of curvature of the wafer before and after film deposition and allows us to calculate the stress. We used Toho machine, for doing the residual stress measurements. The machine is measuring the radius of curvature. The residual stress is calculated by the Stanley's formula: [16]

$$\sigma = \frac{E_{subst}}{6(1-\nu_s)} \frac{t_s^2}{t_f} = \left[\frac{1}{R} - \frac{1}{R_0} \right] \quad (2)$$

where E_{subst} is the Young's modulus, ν_s is the Poisson's ratio and t_s and t_f are the thickness of the substrate and film, R and R_0 are the radius of curvature of the substrate after and before deposition. In our case the thickness of the substrate is the thickness of the Si wafer, $t_s = 525 * 10^6$ [nm]. The value of the Young's modulus and the Poisson's ratio together is $\frac{E_{subst}}{(1-\nu_s)} = 1,805 * 10^{11}$ [Pa]. The positive sign of the radius of curvature corresponds to a concave surface, whereas negative signs to a convex one.



Figure 12. Toho technology FLX 2320



Figure 13. KLA Tencor OmniMap RS75

The stress measured on Toho, for the only aluminum layer wafers is:

$$\begin{aligned}\sigma_{AlN(62539)} &= -3461,12 \pm 102,88 \\ \sigma_{AlN(62543)} &= -3601,80 \pm 20,03\end{aligned}\tag{3}$$

4.5 KLA Tencor OmniMap RS75

The resistivity meter four-point measurement tool, KLA Tencor OmniMap RS75, presented on figure 13, is placed in zone 4 inside the clean room. We used this machine to measure the resistivity of the Pt layer using the Pt probe from the system.

4.6 XRD

The XRD machine, presented on figure 14, is placed in a Lab outside the clean room. We used this machine, for obtaining the crystallinity of the aluminum nitride and platinum layers. The Bragg's law is used in the system of the machine to calculate details about the crystal structure. The XRD measurements were performed by Mr. Kaitlin Howell. The calibration of the z-axis was fixed (which is the max and min that the machine can go -1 to 1) on such way that we find the angle in which 50 % of the x-rays are diffracted. We assume, that is is the perfect height for measuring the wafer. Than on top of that, for that fixed height (angle), we find and save the angle in which there is a pick. The pick means that we touched a grating and we diffracted from it. In the data base of the XRD machine, there are stored specific pick values for each material. Thus, we know and expect where the pick should approximately appear for Si, Pt, AlN and Al. For example, for Si, the angle (2θ) between the tube (x-ray producer) and the detector (CCD camera) is $2\theta = +68$ degrees. This is the angle where the pick appears specifically for Si. We measure only the pick of the second layer AlN, because we are only interested in this active layer of AlN. Additionally, the gratings may not be perpendicular to the xy-plane and we perform another calibration on top of the previous one, by finding another two angles θ_1 (angle between the x-axis and the tube) and θ_2 (angle between the x-axis and the detector) which are not the same now. This two angles are slightly different, but their sum should be equal to 2θ angle. In the final step of the calibration we calibrate around the y-axis by making the wafer measure the biggest pick. The biggest pick is always when the wafer is flat, hence we try to put the wafer in flat position. For each wafer, we should make different calibration because Si wafers are not perfect rather with some standard deviation.



Figure 14. XRD machine

4.7 Procedure for measuring thickness

Since we can measure the aluminum nitride layer thickness, t_{AlN} on Sopra Ges 5e, we need to find a way to measure the total thickness of the two layers of aluminum nitride and platinum layers together, t_{AlN+Pt} , in terms to eventually be able to calculate the platinum thickness as:

$$t_{Pt} = t_{AlN+Pt} - t_{AlN} \quad (4)$$

For measuring the total thickness of the two layers of aluminum nitride and platinum layers together, t_{AlN+Pt} , we apply and remove a tape and ink before and after the deposition of the layers. When taking the tape off, ideally, we aim to remove aluminum nitride and platinum layers, without taking out the SiO_2 layer. The step measured with the Dektak machine is exactly the total thickness of the two layers of aluminum nitride and platinum layers together, t_{AlN+Pt} . The applied tape is flipped on one side, for easy removal. Due to the diversity of tapes that we could've possibly use in the clean room, we weren't sure which one is most suitable. On wafer number 62545, we applied scotch tape but on wafers number 62540 and 62546, we applied kapton tape. The scotch tape, shown on figure 15, after the deposition was burned, damaged and hard to remove from the wafer. However the kapton tape, remained not damaged after the deposition since is thermally stable and removing the kapton tape with hand was successful but still with some residues. As we already mentioned before, the SiO_2 layer thickness was premeasured at the place of the tape and the results confirmed that the SiO_2 layer was not removed by removing the tape.

Note: Don't use any other tape, always use only Kapton tape!

Moreover, we applied both tape and ink with marker pen on the rest of the wafers and the prepared wafers before the deposition of aluminum nitride and platinum layers looked like on figure 16. For removing residues from both the tape and ink, we used the plade solvent photolithography wet bench Z1, placed in zone 1. [17] Firstly, we immerse the wafer in a container filled with isopropanol and second, we place the container into the ultrasonic tank. The process time for removing the residues from the tape was around 20 min, since the tape

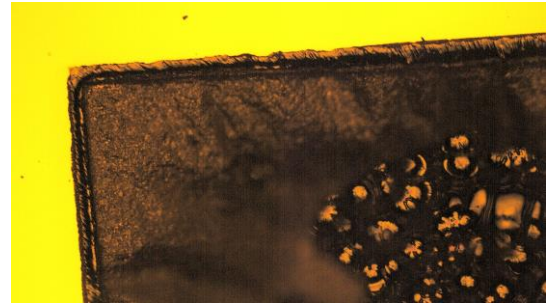


Figure 16. Top left corner of the tape on wafer number 62545

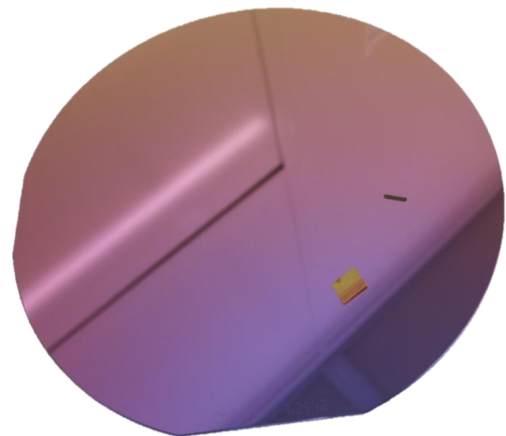


Figure 15. Prepared wafer before deposition

area is quite large. Removing the ink was achieved with process time of around 5 min for each wafer since the ink area is smaller than the tape area. We learned that the wafer, should be placed in vertical position in the container, otherwise the residues can't fall at the bottom of the container without sticking everywhere to the whole surface of the wafer. We used vertical container for this purpose. Despite this, acetone is not recommended for cleaning the residues. Instead, it's better to use isopropanol. Finding a good place to measure was easier for some wafers than to others. Significantly, the thickness results were different for different places on the tape or ink. At this point we learned the importance of looking at the microscope before doing the Dektak measurements in terms of finding a clean and suitable place on the tape or ink for measuring the step. Eventually we manage to find good place to measure on each wafer, either on the tape or on the ink.

Note: Look at the microscope before doing the profilometer measurements!

After looking at the microscope, we observed that the ink surface is much cleaner if we apply thin layer of the ink as shown on figure 15. Furthermore, applying the ink is easier and faster than applying the tape. Still, if one apply big amount of ink (many times with the marker) the ink removal is not successful, even after a long processing time in the ultrasonic bath. On the other hand, if one apply thin layer of ink, will be able to perfectly remove the ink. As we can notice at the microscope pictures, the most cleaned tape, is not looking as clean as the most cleaned ink. Some edges at the tape, still have some residues, even after long process time at the ultrasound. Indeed, the surface with ink is cleaner than the one with the tape, for most of the wafers.

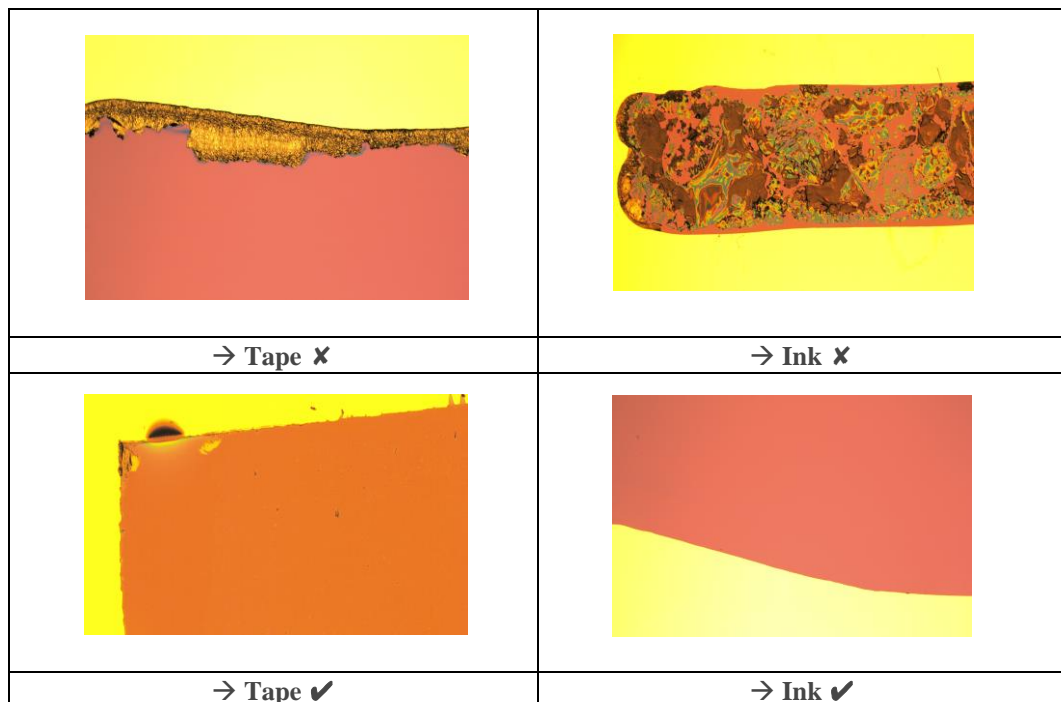


Figure 17. Microscope pictures from good and bad places at tape and ink

Note: Ink is the better choice, if you apply it properly (only twice with the marker)!

After finding good place to measure, the measurements were performed. For the wafers 62545, 62540 and 62546, the measurements were conducted on three different resolutions, listed in table 1, since we weren't sure which resolution is acceptable in our case. Doing the Dektak measurement on these three wafers was easier than the other, because there was bigger and cleaner area at the tape.

Resolution [$\mu\text{m}/\text{Pt}$]	Length[μm]	Duration [s]
0,044	800	60
0,033	1000	100
0,022	500	80

Table 1. Resolutions for Dektak measurements

In order to conclude which resolution is the best, the thickness data was plotted with its STD, shown on figure 18.

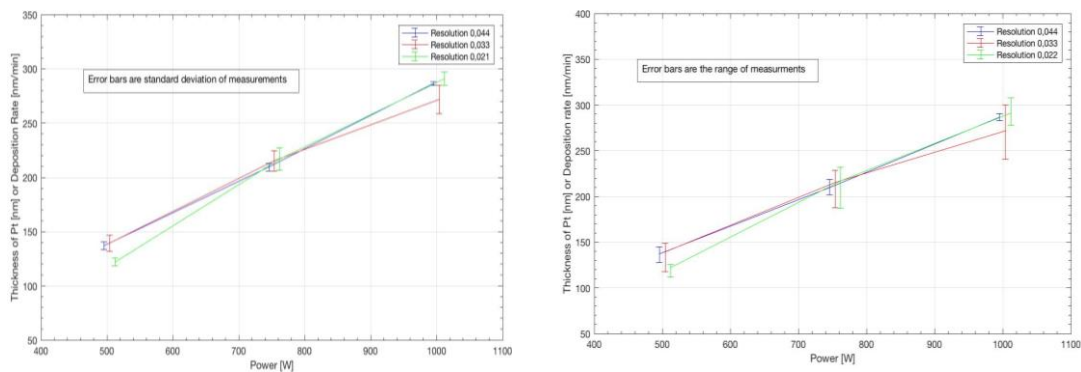


Figure 18. STD (left) and range(right) of Pt thickness of three wafers: 62540, 62546 and 62545, deposited on three different target powers, measured at three different resolutions: 0.044, 0.033 and 0.022

As we can see from the graphs, all the resolutions give almost the same values for the thickness. Because the resolution 0.044 has the least amount of error, we assume this resolution for the rest of the report and the next deposited wafers, were only measured with this resolution.

5 RESULTS

5.1 Results of thickness measurements

The data from the thickness measurements is given in the appendix. For each wafer, we made four measurements of the thickness on the Dektak machine: $t_{\text{AlN+Pt}}^i$, where $i=1,2,3,4$. Then the average thickness and the standard deviation of the thickness were calculated. The standard deviation and the range of the platinum thickness, shown on figure 19, are plotted for three

different powers and three different gas flows. Moreover, in figure 20, we present the thickness of all four layers which is following the same trend as the thickness of only platinum thickness.

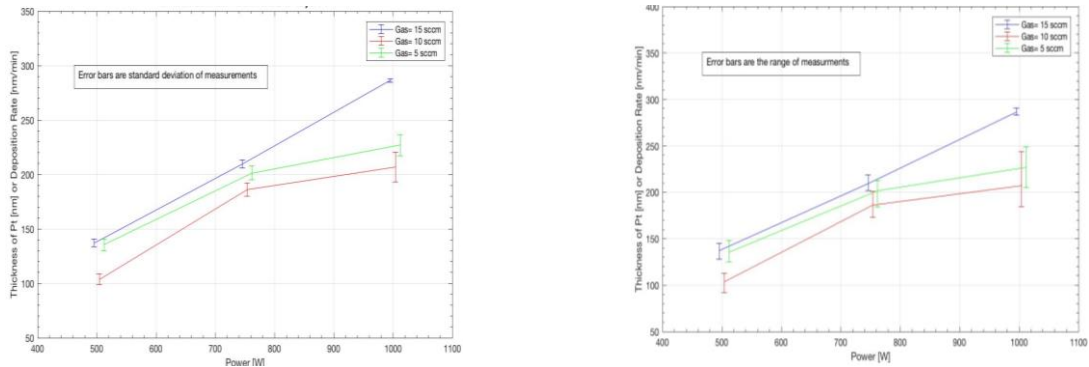


Figure 19. STD (left) and range (right) of platinum thickness, measured at best resolution

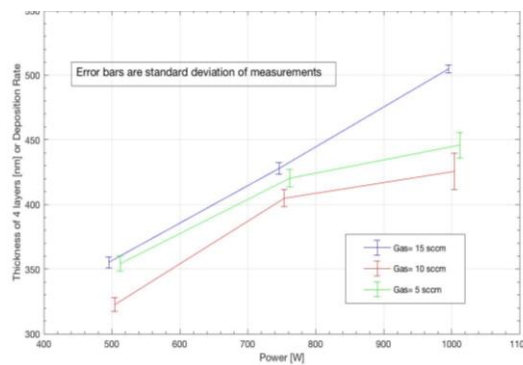


Figure 20. STD of AlN+Pt+AlN+AL thickness of nine wafers, measured at best resolutions

5.2 Results of stress measurements

All values of the radius of curvature measured for all wafers, are shown in the appendix. The stress of the seed aluminum nitride and platinum layer, is σ_{AlN+Pt} , and it was calculated by taking the average of the four measurements results (twice in two directions) from the Toho, for each wafer. The four measurements are denoted as σ_{AlN+Pt}^i , where $i=1,2,3,4$. Then, the average thickness and the STD, for each wafer was calculated. Since we can't measure the Pt stress directly with any machine, we need to calculate it. The Pt stress, can't be calculated simply by subtracting the total stress in the aluminum nitride and platinum layers with the stress in the aluminum nitride layer, but the thickness is also included in the formula:

$$\sigma_{pt} = \frac{\sigma_{AlN+Pt} t_{AlN+Pt} - \sigma_{AlN} t_{AlN}}{t_{pt}} \quad (5)$$

Similarly, we can't measure the only the active aluminum nitride and aluminum layers' stress directly with any machine and we need to also calculate it. The stress on these two final layers, can't be calculated simply by subtracting the total stress in the four layers with the stress in the seed aluminum nitride and platinum layers, but the thickness is also included in the formula:

$$\sigma_{AlN+Al} = \frac{\sigma_{4layers} t_{4layers} - \sigma_{AlN} t_{AlN} - \sigma_{Pt} t_{Pt}}{t_{AlN+Al}} \quad (6)$$

The standard deviation and the range of platinum stress, shown on figure 21, are plotted for three different powers and three different gas flows. On figure 22, the residual stress of platinum layer is plotted as a function of the platinum thickness. The shape symbols on the graph represent the powers:

- = 1000 W
- ▲ = 750 W
- = 500 W

The colors on the same graph represent the gas flows:

- black = 15 sccm Ar
- blue = 10 sccm Ar
- green = 5 sccm Ar

On the figure 21, we can notice that if we increase the power the compressive stress of the Pt layer decreases with linear behavior. There is very small change in the stress between the wafers deposited on 750 [W] and 1000 [W].

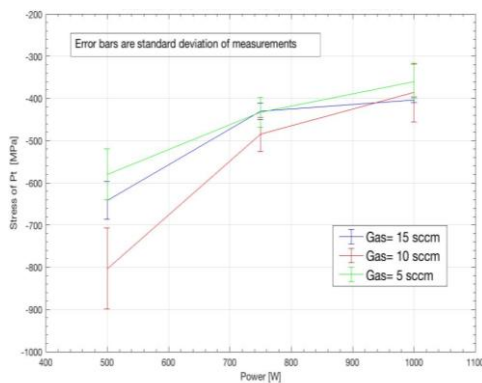


Figure 21. Platinum Stress and STD versus power for different gas flows

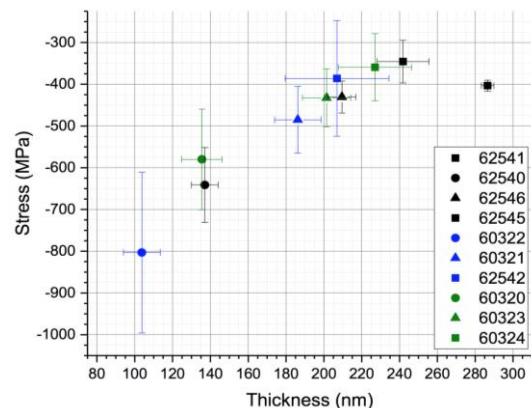


Figure 22. Residual stress in platinum layer versus thickness

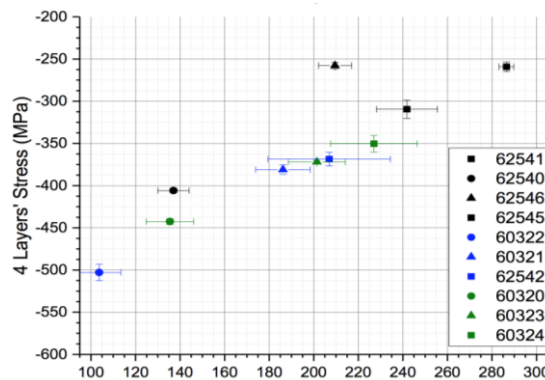


Figure 23. Residual stress in 4 layers versus thickness

5.3 Results of resistance and resistivity measurements

The resistance of a given material increases with length, but decreases with increasing cross-sectional area. From the above equations, resistivity has the unit ($\Omega \cdot \text{m}$). We used Omnimap for measuring the resistivity. In the table we listed the measured values at 5 points at the Pt surface. Then, we calculated the resistivity ρ , which is a property that quantifies how strongly a given material opposes the flow of electric current, by the formula:

$$\rho = t_{Pt} R \quad (7)$$

The resistance of the platinum layer, shown in figure 24, is plotted versus the power. Furthermore, in figure 25, we are presenting the resistivity of the platinum layer as a function of the power. Additionally, in figure 26, the resistivity versus the thickness of the platinum layer is shown. As mentioned above, the shape symbols on the graph represent the powers:

- = 1000 W
- ▲ = 750 W
- = 500 W

The colors on the same graph represent the gas flows:

- black = 15 sccm Ar
- blue = 10 sccm Ar
- green = 5 sccm Ar

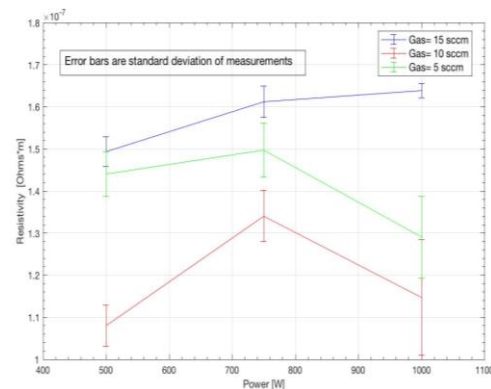
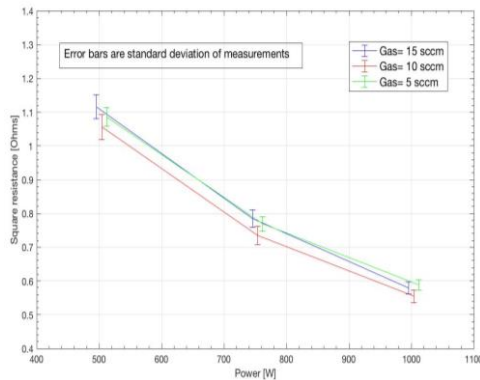


Figure 25. Square resistance of platinum Figure 24. Resistivity of platinum layer

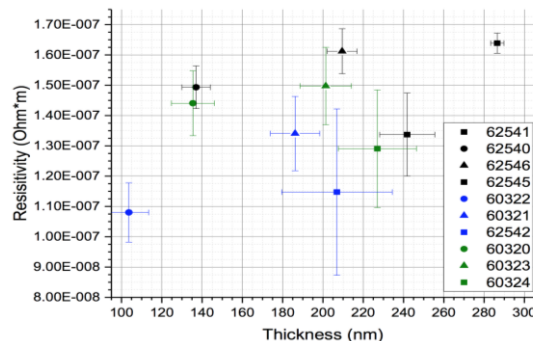


Figure 26. Resistivity versus thickness of platinum layer

5.4 Results of XRD measurement

In figure 26, we are presenting the rocking curve of AlN FWHM versus the thickness of the platinum layer, to see if there is difference in AlN and in Pt crystal lattice. Moreover, in figure 27, the Pt FWHM versus the thickness of the platinum layer is shown. Similarly, the shape symbols on the graph represent the powers:

- = 1000 W
- ▲ = 750 W
- = 500 W

The colors on the same graph represent the gas flows:

- black= 15 sccm Ar
- blue= 10 sccm Ar
- green= 5 sccm Ar

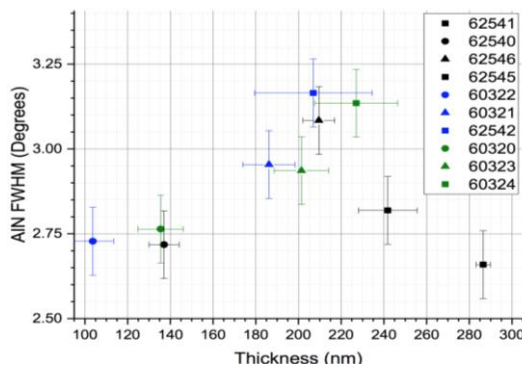


Figure 28. Rocking curve of AlN FWHM versus thickness of platinum

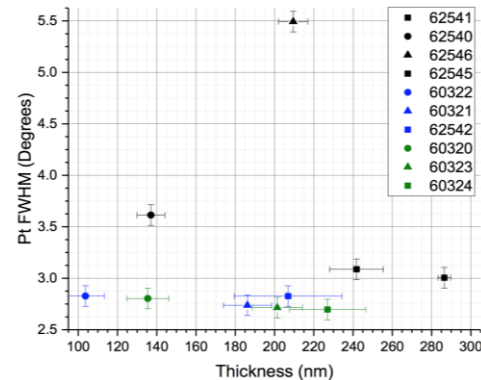


Figure 27. Rocking curve of Pt FWHM versus the thickness of platinum layer

Gaussian fitting was made to the results and the data was extracted. The data from the XRD measurements, in figure 29, is showing the rocking curve of platinum as function of the deposition conditions. Additionally, in figure 30, we are plotting the rocking curve of aluminum nitride for different powers and gas flow.

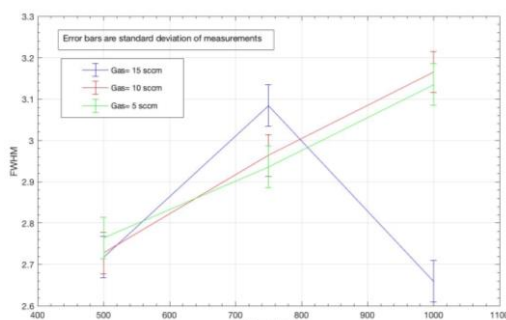


Figure 29. Rocking curve of platinum for different deposition parameters

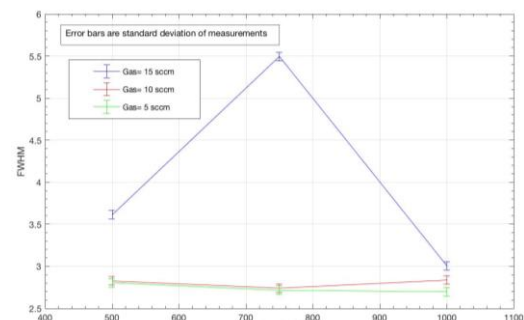


Figure 30. Rocking curve of aluminum nitride for different deposition parameters

6 DISCUSSION

Since we desire the slowest deposition rate while still having a stable and reproducible rate, we keep the deposition time constant and all the wafers were deposited for the same deposition time. But we were changing the thickness, by changing some of the parameters in the Spider machine, to be more exact the power and the gas. As we can see on figure, for gas of 15 [sccm], we have thicker Pt layer, than the one for gas of 10 and 5 [sccm]. Surprisingly, when we apply gas of 5 [sccm] we have thicker Pt layer than when we apply 10 [sccm]. Because of this results we made the 2nd deposition where we deposited two wafers with 500 [W]/10 [sccm] and 500 [W]/5 [sccm] to see if the results will be the same. The wafers deposited on 5 and 10 [sccm] follow the same trend of the thickness. When increasing the power from 500 [W] to 750 [W] there is clear increase in the Pt thickness. If we increase the power, and we don't have enough argon gas (10 or 5 sccm) we notice no increase in the deposition rate. No matter how much we increase the power it is not enough because we have only certain amount of Ar gas for the deposition. Thus, there is no increase in the deposition rate. The results clearly indicate that the thickness of the platinum thin film is linearly proportional with the power. As the power enlarge, the platinum layer thickness is proportionally growing. The residual stress is the stress caused by the deposition of the layer. In the ideal case, the residual stress is zero and the radius of curvature measured on Toho is also zero. In this case, the wafer has flat surface. If the wafer is not flat, it may have different behavior when we induce the piezoelectric stress. As we can see on figure 21, for power of 500 [W], the stress is dependent on the gas flow. The wafer deposited on gas of 10 [sccm] is the one with maximum stress. However, wafers deposited on 15 and 5 [sccm] are slightly different in the amount of residual stress. For the other powers of 750 [W] and 1000 [W], the different gasses do not change a lot in the platinum stress. The residual stress is also influenced by how much material is deposited, as shown on figure 22. As one increase the thickness of a layer, the residual stress decrease. To that end, both layer thickness and deposition conditions influence the results of the stress. The dependence on the resistivity and the power, shown on figure 24 is linear. With increasing the power, the resistance linearly decreases. On the other hand, the resistance is not dependent on the gas flow, since all values are relatively close to each other. Moreover, the resistivity, shown on figure 25, is dependent on both deposition parameters, but there is not so much behavior, because the error bars are large. As we can see on figure 27,28, 29 and 30, change in power do not significantly influence the crystallinity of the aluminum nitride and platinum layers, since all values for the full width at half maximum (FWHM) are in the range from [2.5, 5.5]. The is odd behavior of the wafer deposited on 750[W] and 15 [sccm], for the crystal lattice of the aluminum nitride. From the rocking curve of Pt, presented on figure 29, we can see that the wafer deposited on 1000[W] and 15 [sccm] makes the biggest difference in the FWHM values. The results from the redeposition for the wafers on 500 [W] and 5 and 10 [sccm] are presented in table 2. After the redepositing we noticed no difference between 5 and 10 [sccm] in the thickness of the platinum layer, since the STD are quite large. The reason for this can

be found in the machine imperfection and it can mean that the machine don't put the gas properly or maybe the plasma inside the deposition machine is not stable.

Wafers:	68135	68136
t_{Pt}	37,08	39,90
Δt_{Pt}	0,69	2,94
σ_{Pt}	-885,02	-864,53
$\Delta \sigma_{Pt}$	27,73	6,01
ρ	1,96E-07	2,01E-07
$\Delta \rho$	2,20E-10	2,94E-09

Table 2. Thickness, stress in resistivity with STD for redeposited wafers

7 CONCLUSION

The whole project mostly took place in the clean room in the Center of Micronanotechnology (CMi). at EPFL. In this project, I learned about the theory behind piezoelectric films and magnetron sputtering, but also how to use the machines in the clean room and the theory behind them. Finally, I analyzed the relevant material properties of the deposited Pt thin films to find the best sputtering conditions for producing the thinnest Pt layer on top of which the AlN that will grow with the best quality on top of it. I would like to thank Mr. Kaitlin Howell for guiding me through this semester project. She has always made herself available for any questions and problems that I've had. I would also like to thank the Professor Dr. Guillermo Villanueva for all the help he was given me throughout the entire semester, but also all the stuff in the clean room that helped for any question concerning the clean room.

8 APPENDIX

8.1 DC magnetron sputtering conditions in the Spider machine

62539:

Depositing AlN layer for wafer 62539 (only AlN layer wafer) → chamber 2 → recipe AlN_T_D-1			
Parameters	Min	Max	Ave.
Gas 2 (N2) [sccm]	39.94	40.05	40.00
Gas 3 (Ar) [sccm]	9.93	10.07	10.00
Pressure	0.00541	0.00566	0.00548
Temperature [°C]	59.1	59.4	59.31
DC Bias [W]	82.52	94.50	90.04
Forward Power [W]	4.43	6.08	5.03
DC Voltage [V]	240	242	240.46
DC Current [A]	6.21	7.05	6.28
DC Power [W]	1497	1706	1510.61
Deposition time[s]	19		

62540:

Depositing AlN layer for wafer 62540 → chamber 2 → recipe AlN_T_D-1			
Parameters	Min	Max	Ave.
Gas 2 (N2) [sccm]	39.95	40.05	40.00
Gas 3 (Ar) [sccm]	9.94	10.06	10.00
Pressure	5.47e-003	5.66e-003	5.52e-003
Temperature [°C]	62.6	62.9	62.72
DC Bias [W]	81.19	94.50	88.67
Forward Power [W]	4.43	5.99	5.15
DC Voltage [V]	237	240	238.32
DC Current [A]	6.26	7.12	6.33
DC Power [W]	1496	1702	1508.51
Deposition time[s]	19		

Depositing Pt layer for wafer 62540 → chamber 3 → Pt_T_D-1			
Parameters	Min	Max	Ave.
Gas 3 (Ar)	14.94	15.09	15.00
Pressure	3.71e-003	3.81e-003	3.73e-003
Temperature	53.3	53.6	53.47
DC Voltage [V]	382	448	443.30
DC Current [A]	0.32	1.13	1.08
DC Power [W]	134	510	485.91
Deposition time [s]	61		

62546:

Depositing AlN layer for wafer 62546 → chamber 2 → recipe AlN_T_D-1			
Parameters	Min	Max	Ave.
Gas 2 (N2) [sccm]	39.96	40.05	40.00
Gas 3 (Ar) [sccm]	9.94	10.08	10.00
Pressure	5.47e-003	5.66e-003	5.52e-003
Temperature [°C]	61	61.3	61.19
DC Bias [W]	81.19	94.50	89.12
Forward Power [W]	3.65	5.82	4.87
DC Voltage [V]	237	240	238.34
DC Current [A]	6.26	7.2	6.33
DC Power [W]	1496	1721	1508.70
Deposition time[s]	19		

Depositing Pt layer for wafer 62546 → chamber 3 → Pt_T_D-1			
Parameters	Min	Max	Ave.
Gas 3 (Ar)	14.94	15.09	15.00
Pressure	3.71e-003	3.86e-003	3.73e-003
Temperature	52.7	53.1	52.94
Voltage [V]	368	478	472.39
Current [A]	0.37	1.58	1.51
Power [W]	139	761	725.34
Deposition time [s]	61		

62545:

Depositing AlN layer for wafer 62545 → chamber 2 → recipe AlN_T_D-1			
Parameters	Min	Max	Ave.
Gas 2 (N2) [sccm]	39.96	40.04	40.00
Gas 3 (Ar) [sccm]	9.94	10.05	10.00
Pressure	5.41e-003	5.66e-003	5.49e-003
Temperature [°C]	59.7	60	59.87
DC Bias [W]	82.52	95.83	90.56
Forward Power [W]	4.17	6.51	5.15
DC Voltage [V]	238	240	239.34
DC Current [A]	6.24	7.03	6.30
DC Power [W]	1497	1688	1508.53
Deposition time[s]	19		

Depositing Pt layer for wafer 62545 → chamber 3 → Pt_T_D-1			
Parameters	Min	Max	Ave.
Gas 3 (Ar)	14.94	15.09	15.00
Pressure	3.73e-003	3.84e-003	3.74e-003
Temperature	52.2	52.7	52.50
DC Voltage [V]	401	509	499.44
DC Current [A]	0.28	2.01	1.90
DC Power [W]	118	1011	968.94
Deposition time [s]	60		

62543:

Depositing AlN layer for wafer 62543 (only AlN layer wafer) → chamber 2 → recipe AlN_D-1			
Parameters	Minimum	Maximum	Average
Gas 2 (N2) [sccm]	39.93	40.04	40.00
Gas 3 (Ar) [sccm]	9.95	10.08	10.00
Pressure	5.44e-003	5.63e-003	5.49e-003
Temperature [°C]	38.9	39	38.90
DC Bias [W]	85.19	97.16	92.39
Forward Power [W]	3.91	6.16	5.07
DC Voltage [V]	238	241	238.88
DC Current [A]	6.26	7.04	6.32
DC Power [W]	1497	1696	1508.86
Deposition time[s]	1		

62541:

Depositing AlN layer for wafer 62541 → chamber 2 → recipe AlN_D-1			
Parameters	Min	Max	Ave.
Gas 2 (N2) [sccm]	39.94	40.04	40.00
Gas 3 (Ar) [sccm]	9.92	10.06	10.00
Pressure	5.41e-003	5.63e-003	5.48e-003
Temperature [°C]	38.7	38.9	38.76
DC Bias [W]	86.52	95.83	91.58
Forward Power [W]	4.17	5.46875	4.93
DC Voltage [V]	237	240	238.35
DC Current [A]	6.25	7.13	6.32
DC Power [W]	1496	1705	1506.27
Deposition time[s]	19		

Depositing Pt layer for wafer 62541- recipe name: Pt_D-1 → chamber 3			
Parameters	Min	Max	Ave.
Gas 3 (Ar)	14.9363	15.0801	15.00
Pressure	3.71e-003	3.79e-003	3.73e-003
Temperature	0	31.7	4.1
DC Voltage [V]	401	500	493.58
DC Current [A]	0.323	2.005	1.93
DC Power [W]	138	1010	969.40
Deposition time [s]	60		

62542:

Depositing AlN layer for wafer 62542 → chamber 2 → recipe AlN_D-1			
Parameters	Min	Max	Ave.
Gas 2 (N2) [sccm]	39.95	40.04	40.01
Gas 3 (Ar) [sccm]	9.93	10.07	10.00
Pressure	5.41e-003	5.63e-003	5.48e-003
Temperature [°C]	38.5	38.6	38.56
DC Bias [W]	85.19	97.16	91.68
Forward Power [W]	3.91	6.77	5.11
DC Voltage [V]	237	239	237.73
DC Current [A]	6.27	7.05	6.34
DC Power [W]	1496	1679	1506.99
Deposition time[s]	19		

Depositing Pt layer for wafer 62542- recipe name: Pt_D-1 → chamber 3			
Parameters	Min	Max	Ave.
Gas 3 (Ar)	9.94	10.08	10.00
Pressure	2.84e-003	2.94e-003	2.86e-003
Temperature	0	31.7	8.99
DC Voltage [V]	387	510	502.30
DC Current [A]	0.276	1.976	1.89
DC Power [W]	112	1013	968.57
Deposition time [s]	60		

60324:

Depositing AlN layer for wafer 60324 → chamber 2 → recipe AlN_D-1			
Parameters	Min	Max	Ave.
Gas 2 (N2) [sccm]	39.96	40.07	40.00
Gas 3 (Ar) [sccm]	9.93	10.09	10.00
Pressure	5.41e-003	5.63e-003	5.47e-003
Temperature [°C]	38.3	38.4	38.38
DC Bias [W]	85.19	95.83	92.01
Forward Power [W]	4.43	5.99	5.03
DC Voltage [V]	237	239	237.83
DC Current [A]	6.27	7.13	6.34
DC Power [W]	1496	1696	1509.38
Deposition time[s]	19		

Depositing Pt layer for wafer 60324- recipe name: Pt_D-1 → chamber 3			
Parameters	Min	Max	Ave.
Gas 3 (Ar)	4.93	5.08	5.00
Pressure	1.86e-003	1.99e-003	1.89e-003
Temperature	31.7	31.8	31.70
DC Voltage [V]	403	530	520.31
DC Current [A]	0.295	1.907	1.83
DC Power [W]	115	1012	969.95
Deposition time [s]	60		

60321:

Depositing AlN layer for wafer 60321 → chamber 2 → recipe AlN_D-1			
Parameters	Min	Max	Ave.
Gas 2 (N2) [sccm]	39.94	40.05	40.00
Gas 3 (Ar) [sccm]	9.93	10.08	10.00
Pressure	5.41e-003	5.63e-003	5.47e-003
Temperature [°C]	38.1	38.2	38.19
DC Bias [W]	82.523	95.83	91.20
Forward Power [W]	3.90	5.642	4.90
DC Voltage [V]	237	239	237.96
DC Current [A]	6.26	7.23	6.34
DC Power [W]	1496	1721	1509.48
Deposition time[s]	19		

Depositing Pt layer for wafer 60321- recipe name: Pt_D-1 → chamber 3			
Parameters	Min	Max	Ave.
Gas 3 (Ar)	9.94	10.08	10.00
Pressure	2.86e-003	2.94e-003	2.87e-003
Temperature	31.7	31.8	31.70
DC Voltage [V]	382	485	478.82
DC Current [A]	0.3	1.56	1.48
DC Power [W]	122	759	724.63
Deposition time [s]	60		

60323:

Depositing AlN layer for wafer 60323 → chamber 2 → recipe AlN_D-1			
Parameters	Min	Max	Ave.
Gas 2 (N2) [sccm]	0	0	0
Gas 3 (Ar) [sccm]	39.95	40.05	40.00
Pressure	9.94	10.08	10.00
Temperature [°C]	5.41e-003	5.63e-003	5.47e-003
DC Bias [W]	38	38.1	38.09
Forward Power [W]	82.52	94.50	90.25
DC Voltage [V]	4.34	6.08	5.24
DC Current [A]	0	0	0
DC Power [W]	237	240	238.05
Deposition time[s]	6.26	7.2	6.34
Parameters	1497	1720	1508.77
Gas 2 (N2) [sccm]	19		

Depositing Pt layer for wafer 60323- recipe name: Pt_D-1 → chamber 3			
Parameters	Min	Max	Ave.
Gas 1 (O2)	0	0	0
Gas 2 (N2)	0	0	0
Gas 3 (Ar)	4.94	5.08	5.00
Pressure	1.87e-003	1.98e-003	1.90e-003
Temperature	31.70	31.80	31.75
Bias	Not used		
DC Voltage [V]	399	502	493.97
DC Current [A]	0.33	1.513	1.44
DC Power [W]	138	761	725.17
Deposition time [s]	61		

60322:

Depositing AlN layer for wafer 60322 → chamber 2 → recipe AlN_D-1			
Parameters	Min	Max	Ave.
Gas 2 (N2) [sccm]	39.96	40.04	40.00
Gas 3 (Ar) [sccm]	9.94	10.07	10.00
Pressure	5.41e-003	5.66e-003	5.47e-003
Temperature [°C]	37.9	38	37.91
DC Bias [W]	82.52	95.83	90.29
Forward Power [W]	3.91	5.82	4.94
DC Voltage [V]	237	240	238.21
DC Current [A]	6.26	7.23	6.33
DC Power [W]	1496	1729	1509.39
Deposition time[s]	19		

Depositing Pt layer for wafer 60322- recipe name: Pt_D-1 → chamber 3			
Parameters	Min	Max	Ave.
Gas 3 (Ar)	9.94	10.09	10.00
Pressure	2.86e-003	2.94e-003	2.87e-003
Temperature	31.7	31.8	31.80
DC Voltage [V]	386	455	449.97
DC Current [A]	0.34	1.11	1.06
DC Power [W]	139	509	486.09
Deposition time [s]	60		

60320 :

Depositing AlN layer for wafer 60320 → chamber 2 → recipe AlN_D-1			
Parameters	Min	Max	Ave.
Gas 2 (N2) [sccm]	39.96	40.05	40.00
Gas 3 (Ar) [sccm]	9.92	10.08	10.00
Pressure	5.41e-003	5.66e-003	5.48e-003
Temperature [°C]	37.7	37.9	37.80
DC Bias [W]	82.52	95.83	90.68
Forward Power [W]	3.99	6.86	5.12
DC Voltage [V]	237	240	238.20
DC Current [A]	6.26	7.14	6.33
DC Power [W]	1497	1706	1507.82
Deposition time[s]	19		

Depositing Pt layer for wafer 60320- recipe name: Pt_D-1 → chamber 3			
Parameters	Min	Max	Ave.
Gas 3 (Ar)	4.94	5.09	5.00
Pressure	1.87e-003	1.97e-003	1.90e-003
Temperature	0	31.8	21.67
DC Voltage [V]	393	465	459.71
DC Current [A]	0.33	1.08	1.04
DC Power [W]	139	509	485.98
Deposition time [s]	60		

8.2 Raw data thickness measurements

Measured AlN+Pt thickness for different resolution	62540	62546	62545
$t_{\text{AlN+Pt}}^i$ Resolution=0,044 [nm/Pt]	163	220	301
	157	224	305
	155	230	309
	146	237	304
Ave. from resolution=0,044	155,25	227,75	304,75
$t_{\text{AlN+Pt}}^i$ Resolution=0,033 [nm/Pt]	136	238	280
	162	247	259
	167	243	318
	165	206	303
Ave. from resolution=0,033	157,5	233,5	290
$t_{\text{AlN+Pt}}^i$ Resolution=0,021 [nm/Pt]	144	236	309
	143	249	306
	130	250	296
	144	205	326
Ave. from resolution=0,022	140,25	235	309,25

Calculated Pt thickness for different resolution	62540	62546	62545
t_{Pt}^i Resolution=0,044 [nm/Pt]	144,8	201,8	282,8
	138,8	205,8	286,8
	136,8	211,8	290,8
	127,8	218,8	285,8
Ave. from resolution=0,044	137,05	209,55	286,55
t_{Pt}^i Resolution=0,033 [nm/Pt]	117,8	219,8	261,8
	143,8	228,8	240,8
	148,8	224,8	299,8
	146,8	187,8	284,8
Ave. from resolution=0,033	139,3	215,3	271,8
t_{Pt}^i Resolution=0,021 [nm/Pt]	125,8	217,8	290,8
	124,8	230,8	287,8
	111,8	231,8	277,8
	125,8	186,8	307,8
Ave. from resolution=0,022	122,05	216,8	291,05

Note: The thickness is in [nm], the stress is in [Mpa] and the resistance is in [Ohm*m]

Measured AlN+Pt thickness for best resolution	62541	62540	62546	62545	60322	60321	62542	60320	60323	60324
$t_{\text{AlN+Pt}}^i$ $i=1,2,3,4$	259,20	163,00	220,00	301,00	132,00	191,80	262,60	167,00	202,90	255,20
	279,80	157,00	224,00	305,00	111,00	199,10	230,60	147,00	231,40	267,50
	255,80	155,00	230,00	309,00	129,00	220,00	203,10	144,00	228,00	223,60
	247,60	146,00	237,00	304,00	118,00	209,00	206,60	159,00	218,40	237,00
$t_{\text{AlN+Pt}}$	260,60	155,25	227,75	304,75	122,50	204,98	225,73	154,25	220,18	245,83
$\Delta t_{\text{AlN+Pt}}$	13,69	7,04	7,41	3,30	9,75	12,25	27,45	10,69	12,76	19,40
$t_{4\text{layers}}$	460,60	355,25	427,75	504,75	322,50	404,98	425,73	354,25	420,18	445,83
$\Delta t_{4\text{layers}}$	14,58	8,64	8,94	5,99	10,95	13,23	27,91	11,80	13,71	20,04

Thickness of SiO ₂ layer [nm] measured on NanoSpec 6100	62541	62540	62546	62545	60322	60321	62542	60320	60323	60324
Ave. Thickness of SiO ₂	281,59	289,2	285,1	286,5	286,39	285,23	281,19	284,84	285,43	285,72
Max Thickness	283,30	296,6	287,4	291,3	293,20	288,60	282,90	288,00	289,30	282,20
Min Thickness	279,60	287,0	285,7	284,5	282,30	282,10	279,40	281,90	282,30	189,40
STD	10,69	25,01	9,01	12,2	29,38	19,18	10,15	18,31	19,88	18,33
Uniformity[%]	0,66	-	-	-	1,90	1,14	0,62	1,07	1,23	1,26

8.3 Raw data stress measurements

wafer	direction	R _{SiO2}	R _{AIN+Pt}	R _{4 layers}
62541	1	110,63	-108,93	-129,61
	1	111,43	-108,88	-131,08
	2	-5785,00	-54,25	-55,96
	2	-8708,00	-54,26	-56,08
62540	1	81,32	-154,78	-193,48
	1	81,08	-154,94	-193,18
	2	331,27	-68,42	-70,06
	2	332,44	-68,45	-70,02
62546	1	-202,40	-42,97	-54,39
	1	-205,57	-42,98	-54,50
	2	-542,39	-48,90	-66,59
	2	-520,98	-48,83	-66,68
62545	1	-389,13	-41,24	-53,56
	1	-385,54	-41,15	-53,61
	2	-434,32	-42,28	-56,33
	2	-441,49	-42,20	-56,26
60322	1	-838,84	-52,55	-48,98
	1	-863,29	-52,64	-49,00
	2	-818,11	-50,45	-47,35
	2	-789,72	-50,50	-47,32
60321	1	-3364,00	-51,05	-52,19
	1	-3027,00	-51,04	-52,25
	2	639,41	-58,01	-59,46
	2	639,92	-57,90	-59,46
62542	1	66,11	-303,33	-241,66
	1	66,14	-308,65	-238,87
	2	338,40	-70,25	-64,14
	2	340,49	-70,20	-63,91
60320	1	-801,83	-52,58	-49,30
	1	-794,12	-52,59	-49,29
	2	-735,19	-53,03	-49,69
	2	-740,39	-53,05	-49,66
60323	1	-3820,00	-53,02	-52,11
	1	-5056,00	-52,66	-52,30
	2	1703,00	-55,45	-55,00
	2	1623,00	-55,52	-55,09
60324	1	-3820,00	-53,02	-52,11
	1	-5056,00	-52,66	-52,30
	2	1703,00	-55,45	-55,00
	2	1623,00	-55,52	-55,09

wafer	direction	σ_{SiO2}	σ_{AIN+Pt}	$\sigma_{4 layers}$
62541	1	-	-579,72	-301,62
	1	-	-577,76	-298,89
	2	-	-581,05	-318,59
	2	-	-582,71	-318,95
62540	1	-	-1001,85	-407,66
	1	-	-1003,44	-408,70
	2	-	-941,81	-403,62
	2	-	-940,95	-403,53
62546	1	-	-667,43	-260,63
	1	-	-669,95	-261,40
	2	-	-677,46	-255,38
	2	-	-675,66	-253,49
62545	1	-	-589,77	-264,47
	1	-	-590,58	-263,79
	2	-	-580,96	-253,83
	2	-	-583,12	-254,77
60322	1	-	-1207,32	-494,29
	1	-	-1207,47	-494,98
	2	-	-1259,02	-511,56
	2	-	-1254,56	-510,83
60321	1	-	-780,38	-386,22
	1	-	-779,24	-385,13
	2	-	-760,58	-376,39
	2	-	-761,91	-376,34
62542	1	-	-676,72	-375,19
	1	-	-674,45	-376,04
	2	-	-631,48	-361,23
	2	-	-631,13	-361,95
60320	1	-	-955,25	-445,62
	1	-	-954,38	-445,41
	2	-	-940,55	-439,19
	2	-	-940,67	-439,76
60323	1	-	-700,38	-373,57
	1	-	-707,77	-373,40
	2	-	-701,23	-370,37
	2	-	-701,46	-370,35
60324	1	-	-700,38	-373,57
	1	-	-707,77	-373,40
	2	-	-701,23	-370,37
	2	-	-701,46	-370,35

Stress and STD	62541	62540	62546	62545	60322	60321	62542	60320	60323	60324
σ_{Pt}	-345,79	-641,46	-430,44	-403,50	-803,29	-485,13	-386,04	-580,01	-432,53	-359,53
$\Delta\sigma_{Pt}$	51,02	89,82	38,25	13,33	192,49	80,08	138,30	120,48	69,56	80,80
σ_{AlN+Pt}	-580,31	-972,01	-672,63	-586,10	-1232,09	-770,53	-653,45	-947,71	-702,71	-607,10
$\Delta\sigma_{AlN+Pt}$	2,09	35,38	4,72	4,79	28,57	10,75	25,58	8,21	3,40	4,09
$\sigma_{4layers}$	-309,51	-405,88	-257,73	-259,21	-502,91	-381,02	-368,60	-442,49	-371,92	-350,30
$\Delta\sigma_{4layers}$	10,75	2,69	3,89	5,70	9,57	5,39	8,11	3,50	1,81	9,86
σ_{AlN+Al}	43,33	33,58	214,74	238,89	-56,29	18,18	-47,12	-52,84	-7,77	-34,67
$\Delta\sigma_{AlN+Al}$	77,49	72,35	50,40	36,24	114,48	88,24	163,73	94,40	83,21	109,18

Resistance and resistivity	62541	62540	62546	62545	60322	60321	62542	60320	60323	60324
5 points	0,49926	0,97901	0,69298	0,5168	0,93595	0,64790	0,49663	0,95802	0,67263	0,51381
	0,57541	1,0996	0,77017	0,58944	1,08020	0,75807	0,57542	1,09470	0,77862	0,57742
	0,56792	1,1312	0,81183	0,58873	1,08210	0,74059	0,56761	1,08580	0,76863	0,58859
	0,56436	1,1225	0,78736	0,58519	1,05620	0,73473	0,55414	1,05960	0,75681	0,58683
	0,55756	1,1157	0,78426	0,57932	1,05190	0,71856	0,57813	1,11800	0,74093	0,57483
R	0,552902	1,089602	0,76932	0,571896	1,04127	0,71997	0,554386	1,063224	0,743524	0,568296
ΔR	0,03067	0,06289	0,04523	0,03106	0,06044	0,04269	0,0336	0,06241	0,04205	0,03102
ρ	1,33708E-07	1,4933E-07	1,61211E-07	1,63877E-07	1,08011E-07	1,34062E-07	1,14733E-07	1,44046E-07	1,49749E-07	1,29034E-07
$\Delta\rho$	1,36948E-08	7,04182E-09	7,41072E-09	3,30418E-09	9,74698E-09	1,22482E-08	2,74541E-08	1,0689E-08	1,27647E-08	1,94039E-08

Bibliography

- [1] Marc-Alexandre Dubois and Paul Muralt, Stress and piezoelectric properties of aluminum nitride thin films deposited onto metal electrodes by pulsed direct current reactive sputtering, Ceramic Laboratory, Material Science, EPFL Swiss Federal Institute of Technology, 1015 Lausanne, Switzerland, Journal of applied physics, Volume 89, Number 11, 1 June 2001.
- [2] E.H.Sondheimer, Adv.Phys.1 1952 1.
- [3] Y.Namba, Jpn.J.Appl.Phys.9 (1970) 1282.
- [4] A.F. Mayadas, M.Shatzkes, Phys.Rev.B 1 (1970) 1382
- [5] <https://www.memsnet.org/mems/processes/deposition.html>
- [6] Thin Film Growth Through Sputtering Technique and Its Applications, Edgar Alfonso, Jairo Olaya and Gloria Cubillos, National University of Columbia
- [7] <http://www.directvacuum.com/sputter.asp>
- [8] Thin Film Growth Through Sputtering Technique and Its Applications, Edgar Alfonso, Jairo Olaya and Gloria Cubillos, National University of Columbia
- [9] MEMS: Fundamental Technology and Applications, Vikas Choudhary, Krzysztof Iniewski
- [10] A comparison of piezoelectric materials for MEMS power generation, H. Bardaweel, O. Al Hattamleh, R Richards, D. Bahr, and C. Richards, The Sixth International Workshop on Micro and Nanotechnology for Power Generation and Energy Conversion Applications, Nov. 29 - Dec. 1, 2006, Berkeley, U.S.A
- [11] Research on the Piezoelectric Properties of AlN Thin Films for MEMS Applications Meng Zhang, Jian Yang, Chaowei Si, Guowei Han, Yongmei Zhao and Jin Ning, Micromachines 2015, 6, 1236-1248; doi:10.3390/mi6091236
- [12] Marc-Alexandre Dubois and Paul Muralt, Stress and piezoelectric properties of aluminum nitride thin films deposited onto metal electrodes by pulsed direct current reactive sputtering, Ceramic Laboratory, Material Science, EPFL Swiss Federal Institute of Technology, 1015 Lausanne, Switzerland, Journal of applied physics, Volume 89, Number 11, 1 June 2001.
- [13] Manbachi, A. & Cobbold, R.S.C. (2011). "Development and Application of Piezoelectric Materials for Ultrasound Generation and Detection". Ultrasound. 19 (4): 187–196.
- [14] <https://cmi.epfl.ch/thinfilms/Spider600.php>
- [15] https://cmi.epfl.ch/metrology/GES_5E.php
- [16] Stoney formula: Investigation of curvature measurements by optical profilometer, Maria Rosa Ardigo, Maher Ahmed, Aurelien Besnard
- [17] <https://cmi.epfl.ch/photo/dev/PladeZ1.php>